

*Bruce K. Menzies*

# A Computer Controlled Hydraulic Triaxial Testing System

---

**REFERENCE:** Menzies, B. K., "A Computer Controlled Hydraulic Triaxial Testing System," *Advanced Triaxial Testing of Soil and Rock, ASTM STP 977*, Robert T. Donaghe, Ronald C. Chaney, and Marshall L. Silver, Eds., American Society for Testing and Materials, Philadelphia, 1988, pp. 82-94.

**ABSTRACT:** A computer controlled hydraulic triaxial testing system is introduced. A desktop computer is linked to a hydraulic triaxial cell via three microprocessor controlled hydraulic actuators and two subsystems, one for the measurement of axial deformation and the other for the measurement of pore pressure. The separate system elements and subsystems are described in detail. The operation of the system is described, and control algorithms are explained with particular reference to  $K_0$  consolidation and swelling and automatic testing rate by controlled hydraulic gradient. System performance is illustrated by reference to published data describing  $K_0$ , stress path, cyclic loading, and triaxial extension tests. The advantages of the system are summarized.

**KEY WORDS:** computer control, digital controller, saturation ramps, isotropic and anisotropic consolidation, conventional tests, triaxial extension,  $K_0$  consolidation and swelling, stress paths, cyclic loading, automatic drained testing rate, data presentation, repeatability, software based

## System Layout

As shown in the schematic diagram in Fig. 1, a desktop computer is linked to a hydraulic triaxial cell via three microprocessor controlled hydraulic actuators called "digital controllers" [1-4]. The controllers precisely regulate pressure and volume change of deaerated water supplied to the cell to control axial load or axial deformation, cell pressure, and back pressure. The system also measures axial deformation indirectly by volume change into the lower chamber of the cell or by direct measurement of displacement using a digital indicator. Pore pressure may be measured by the back-pressure controller (locked for the undrained condition so there is no volume change) or by a solid state pressure transducer plumbed directly into the base pedestal. The digital controllers, pore pressure indicator, axial deformation indicator, printer, and plotter are connected by interface bus cables to the IEEE 488 standard parallel interface of the computer.

## System Elements

### *The Triaxial Cell*

The triaxial compression/extension cell is based on the design of Bishop and Wesley's [5] hydraulic triaxial apparatus for controlled stress path testing developed at Imperial College

<sup>1</sup> Director, GDS Instruments Ltd., Unit 12 Eversley Way, Thorpe Industrial Estate, Egham, Surrey England TW20 8RG.

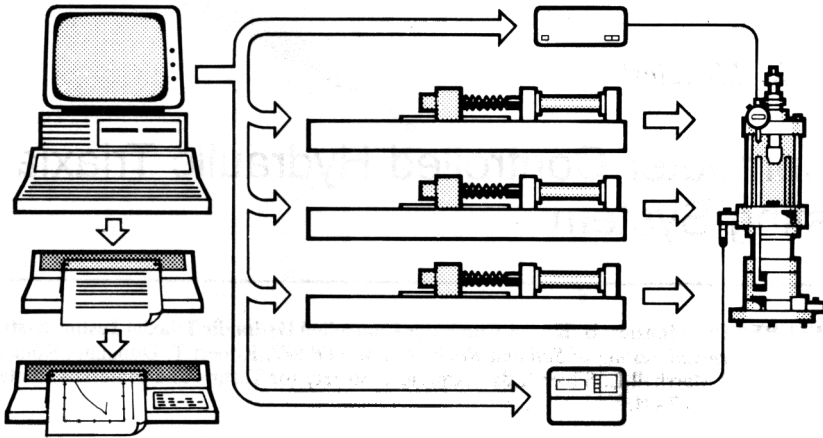


FIG. 1—Diagrammatic layout of the system.

of Science and Technology, London. Note that any test, including a conventional test, may be referred to as a “stress path test.”

Although Bishop and Wesley set out to design “a simple form of triaxial apparatus in which the stress paths encountered in engineering practice can be approximated more readily than in conventional equipment,” their versatile cell is equally adept at carrying out classic “standard” tests as well as advanced tests.

As shown in the schematic diagram in Fig. 2, axial force is exerted on the test specimen by means of a piston fixed to the movable base pedestal. The top cap of the test specimen is fixed in position by an adjustable rod passing through the top of the cell. The piston moves vertically up and down in a linear guide comprising a cage of ball bearings housed in a turret joining the cell to the base. The piston is actuated hydraulically from an integral lower chamber in the base of the cell which contains deaerated water. The piston is sealed into the upper cell and the lower chamber by matched Bellofram rolling diaphragms which sweep equal volumes of water. Accordingly axial ram friction is very small and normally less than 5 kPa of deviator stress.

The statics of the cell are very simple. By considering the equilibrium of the loading ram, the following relationship is obtained:

$$\sigma_a = p(a/A) + \sigma_r(1 - a/A) - W/A \quad (1)$$

where

$\sigma_a$  = the average axial total stress,

$\sigma_r$  = the radial total stress or cell pressure,

$p$  = the pressure in the lower chamber,

$A$  = the current average cross-sectional area of the test specimen (defined as the area of the volumetrically equivalent right cylinder),

$a$  = the effective area of the Bellofram rolling diaphragm, and

$W$  = the weight of the loading ram.

The computer continuously computes the average axial total stress using Eq 1, and so an external or internal load cell is not required and not supplied with the system.

As can be seen from the photograph in Fig. 3, there are two versions of the cell—the

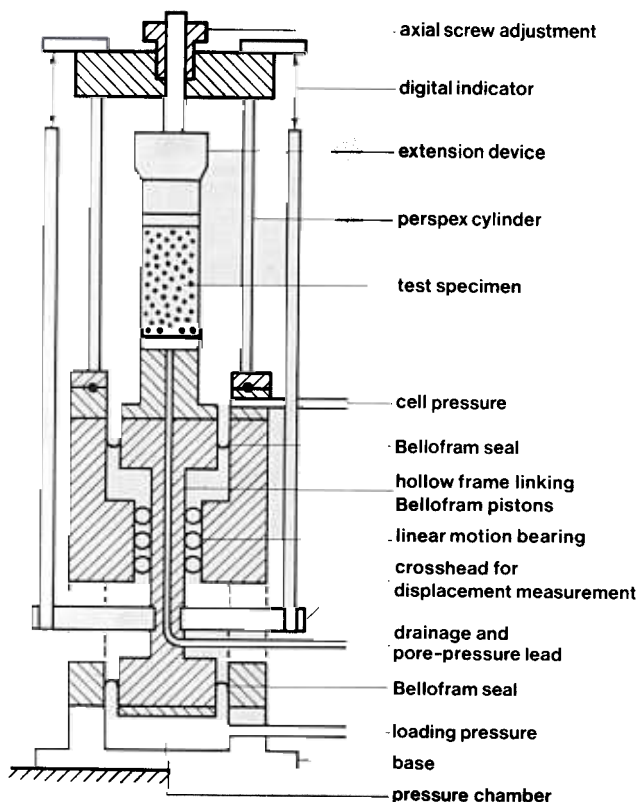


FIG. 2—Diagrammatic layout of the hydraulic triaxial apparatus (after Bishop and Wesley [5]).

smaller one for test specimens of 38-mm diameter, and a larger cell which accommodates 50-, 70-, and 100-mm diameter test specimens by interchangeable base pedestals and top caps.

### *The Extension Device*

The extension device is fitted to the triaxial cells in place of the redundant load cell. The object of the extension device is to allow axial stress to be reduced below radial stress. In conventional triaxial cells this is normally not possible because the radial stress or cell pressure acts vertically on the top cap. Indeed, in many types of conventional cell, a small hole is drilled through the side of the loading ram and into the conical end socket to avoid any possibility of partial pressures between the end of the ram and the ball seating of the top cap. This ensures that the vertical component of cell pressure acts with equal intensity, thus simplifying the statics.

As shown in the schematic diagram in Fig. 4, the hollow adjustable reaction rod passes through the top of the cell. Fixed to the bottom of the rod is a truncated conical fitting which mates with the plane top cap of the triaxial test specimen. The top cap is fitted with a bell mouthed surgical PVC dip molded sleeve.

The cell is filled with water, with air being purged out through the hollow reaction rod.

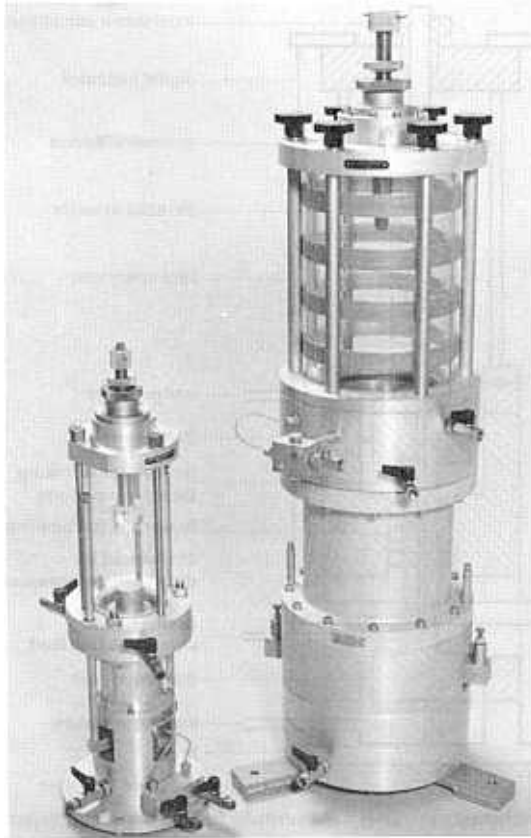


FIG. 3—Hydraulic triaxial cells for test specimen diameters of 38 mm (small) and 50, 70, 100 mm (large) by interchangeable base pedestals and top caps.

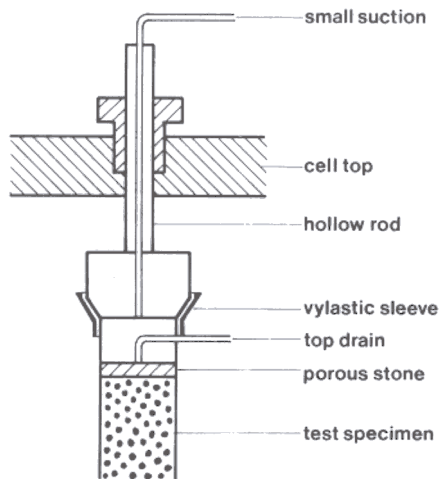


FIG. 4—The extension device.

The reaction rod is then adjusted to dock the plane and conical parts together. Lightly smearing the angled surfaces with soft silicone grease ensures good contact. A small suction can then be applied to the top of the hollow reaction rod to cause the sleeve to seal the interface. Cell pressure is then applied. As the top cap is now sealed to the fixed reaction rod, cell pressure does not act vertically on the test specimen. Accordingly, axial stress can be reduced to below cell pressure.

Provided axial stress always remains positive, there is always a positive load between the mating parts which, therefore, will not move apart. Smooth transitions between compression and extension of course are essential in an advanced triaxial testing system, for example, for stress paths simulating excavations, surcharge removal, emptying of storage tanks, and so forth, or for  $K_0$  consolidation and swelling to a high overconsolidation ratio during SHANSEP procedures.

### *The Digital Controller*

The digital controller shown in the photograph in Fig. 5a is a microprocessor controlled hydraulic actuator for the precise regulation and measurement of liquid pressure and liquid volume change. For the triaxial testing of soils the volumetric capacity is 200 or 1000 cm<sup>3</sup> and the pressure range is 0 to 2000 kPa. Pressure measurement is resolved to 0.2 kPa, and pressure is controlled to 0.5 kPa. For rock mechanics applications the volumetric capacity is nominally 200 cm<sup>3</sup> and the pressure ranges are 7, 10, 20, 32, and 64 MPa.

The principles of operation are shown in the schematic diagram in Fig. 5b. Deaerated water in a cylinder is pressurized and displaced by a piston moving in the cylinder. The piston is actuated by a ball screw turned in a captive ball nut by a stepping motor and gearbox that move rectilinearly on a ball slide.

Pressure is detected by means of an integral solid state pressure transducer. Control algorithms are built into the programmable memory to cause the controller to seek to a target pressure or step to a target volume change. Volume change is measured by counting the steps of the stepping motor. Knowing the number of steps per revolution of the motor, the gearbox ratio, and the pitch of the ball screw, the bore of the pressure cylinder may be found such that one step of the motor equals 1 mm<sup>3</sup>.

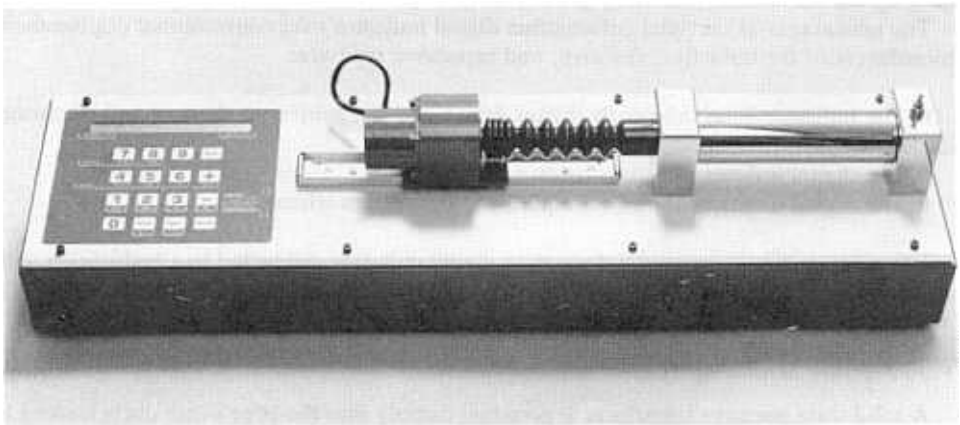


FIG. 5 (a)—Digital controller.

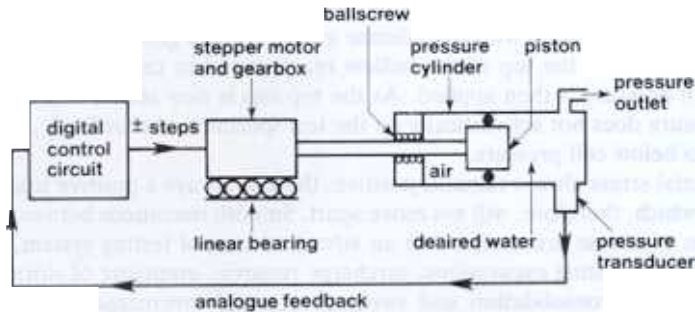


FIG. 5 (b)—Diagrammatic layout of digital controller

In stand-alone mode the instrument is a general purpose constant pressure source, a volume change gauge, a pore pressure measuring system, a flow pump (or screw pump), and a digital pipette. As a constant pressure source it can be used to replace mercury column, compressed air, pumped oil, and dead weight devices. It can be programmed through its own control panel to ramp and cycle pressure and volume change linearly with respect to time.

In computer control mode it is a computer peripheral via the standard IEEE 488 computer interface. The user interface is a control panel comprising a liquid crystal display and membrane touch keypad. This is used in stand-alone mode for entering target pressure, target volume, ramping data, and other functions including access to on-board diagnostics for checking out each of the major hardware components of the system.

### The Axial Deformation Digital Indicator

The axial deformation digital indicator is similar in size and appearance to a conventional dial gauge. In place of the dial is a liquid crystal display. In place of the indicating pointer there is an internal optoelectronic linear encoder and large-scale integration (LSI) counter gauging the movement of a finely graduated glass plate actuated by the external spindle.

The advantages of the axial deformation digital indicator over conventional displacement transducers of the inductive, resistive, and capacitive type are:

- The indicator is an inherently digital device and not subject to thermal and electronic drift.
- The digital indicator displays its own reading.
- The digital indicator does not require any calibration whatsoever.

The subsystem uses an axial deformation digital indicator connected to a multiplexer with an IEEE interface. Axial deformation is resolved to 0.001 mm over a range of 12.7 mm.

### Pore Pressure Measuring System

A solid-state pressure transducer is plumbed directly into the pore water ducts leading to the base pedestal. The transducer is connected to a digital pressure indicator with an IEEE interface. The subsystem resolves pore pressure to  $\pm 0.2$  kPa over a range of 2000 kPa.

## System Operation

### *Test Control*

Continuously and at a frequency typically less than once a second, the computer:

- takes a set of readings from the digital controllers and the axial deformation and pore pressure measuring subsystems,
- calculates the current test parameters and stores them as required, and
- gives new commands to the digital controllers to keep the selected test on the chosen stress path or strain path.

Using this general approach in a series of standard subroutines, a range of tests can be made available by selection from a test menu.

### *Test Menu*

The test menu of the system is as follows:

- saturation by simultaneous ramps of cell pressure and back pressure;
- incremental and ramped evaluation of pore pressure parameter  $B$ ;
- isotropic and anisotropic consolidation;
- unconsolidated-undrained compression/extension;
- consolidated-undrained compression/extension with pore pressure measurement;
- consolidated-drained compression/extension, volume change resolved to  $1 \text{ mm}^3$ ;
- $K_0$  consolidation and swelling for saturated soils;
- continuous linear stress paths, mixed drained and undrained, mixed compression and extension;
- cyclic loading by axial stress controlled square, sinusoidal, and triangular wave forms; periods down to sea wave periods; and
- permeability by constant hydraulic gradient or by constant rate of flow [6].

The system has a “loop-round” facility enabling any series of the above tests to be sequentially carried out on the one test specimen with changed height and diameter being passed on from the end of one test to the beginning of the other, for example, unconsolidated-undrained after  $K_0$  gives a SHANSEP capability.

### *Test Control Algorithms*

The on-board intelligence of the digital controller provides useful functions (seek to target pressure, step to target volume change, ramp pressure, ramp volume change) which facilitate the design of the test control algorithms. Generally, for tests most simply described by a stress path, the controllers are continually set and reset to ramped pressure control (for a stress path test per se, this refers to the axial and radial stress controllers). For tests most simply described by a strain path (for example, a U-U test) the controllers are continually set and reset to ramped volume change control (for the U-U test this would be the axial controller only). There are two notable exceptions to this approach— $K_0$  consolidation and swelling, and automatic drained testing rate by controlled hydraulic gradient, as discussed below.

### *K<sub>0</sub> Consolidation and Swelling*

Here the test control rule is that the volume change in the pore water duct must at all times be equal to the volume of the axial deformation times the original average cross-sectional area. This rule is only applicable to saturated soils. Continuously, and at a frequency typically less than once a second, the computer:

- calculates the volume of the axial deformation times the original average cross-sectional area;
- commands the back-pressure controller (which is under volume change control) to step an equal and opposite volume change, that is, extract pore water if consolidation is required, infuse water if swelling is required; and
- commands the cell pressure controller to adjust cell pressure to keep the back pressure constant at the predetermined value.

The test is only valid if the chosen testing rate is such that unacceptable excess pore pressures do not develop (for example, during consolidation, it is possible to imagine contraction of the test specimen adjacent to the base porous stone while bulging occurs in the middle third of the test specimen). Accordingly, it is highly desirable to regulate the testing rate by controlling the hydraulic gradient throughout the height of the test specimen as discussed in the following section.

### *Automatic Drained Testing Rate*

One of the biggest problems associated with any form of triaxial testing is the question of testing rate. This is particularly so in effective stress testing, that is, testing where a complete knowledge of the pore water pressure regime is required.

For the particular case of drained tests (conventional, stress path,  $K_0$ ) where a constant back pressure is applied to the base pedestal or to the top cap, if the testing rate is too high the back pressure may be significantly different from the average pore pressure throughout the test specimen. Accordingly, chosen testing rates tend to err on the side of caution and, in many cases, are far too low. This slows down test throughput and reduces productivity.

An alternative is to measure the difference in pore pressure from one end of the test specimen to the other and to control the testing rate to restrict the difference to an acceptable level. As shown in the schematic diagram in Fig. 6, the system applies a constant back pressure to the top drain and measures the pore pressure at the base pedestal. Axial loading can now be controlled such that the difference in end pore pressures—the excess pore pressure—is either a fixed value, say 5 kPa, or, more logically perhaps, a fixed proportion of axial total stress, say 5%. Referring to Fig. 6, these control criteria may be expressed algebraically as

$$u - u_0 = \Delta u = 5 \text{ kPa} \quad (2)$$

or

$$\Delta u / \sigma_a = 5\% \quad (3)$$

In this way the soil is tested at the optimum testing rate for the chosen criteria, automatically adjusting to changing soil conditions such as permeability, while the state of effective stress is continuously controlled and measured.

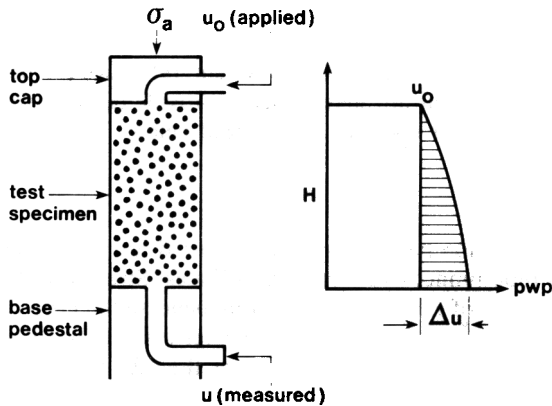


FIG. 6—Diagrammatic representation of variation of pore pressure in a top-drained triaxial test specimen.

### Data Presentation

The system reduces the data into SI units. Optionally, the system can tabulate or plot saved data. The list of parameters available for data presentation are as follows:

- pressure and volume change from each controller,
- time,
- percent axial strain,
- axial stress,
- radial stress,
- effective axial stress,
- effective radial stress,
- deviator stress (Cambridge  $q$ ),
- stress ratio,
- mean stress (MIT  $p$ ),
- mean effective stress (MIT  $p'$ ),
- average radial strain,
- average diameter change,
- pore water pressure,
- volume change,
- change in length,
- square root of time,
- $\log_{10}$  (time),
- $\log_{10}$  (effective axial stress),
- maximum shear stress (MIT  $q$ ),
- maximum shear strain,
- spherical pressure (Cambridge  $p$ ), and
- effective spherical pressure (Cambridge  $p'$ ).

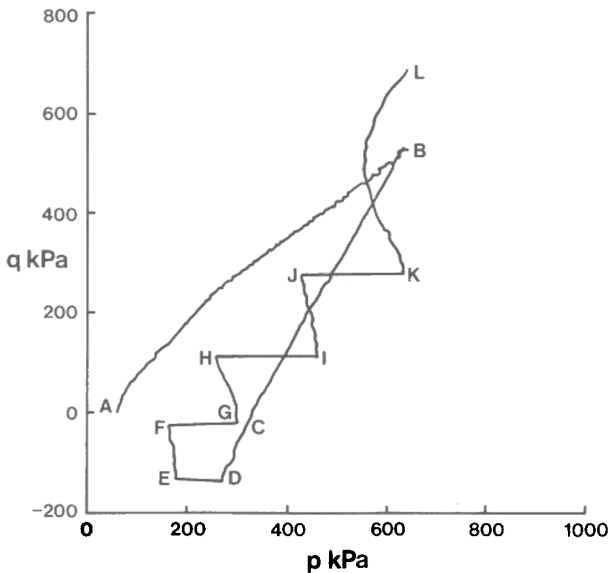
Any one parameter can be plotted against any other. Scaling can be automatic or overridden to allow families of curves to be plotted within the same set of axes or to enlarge particular features. Data can also be smoothed using a cosine weighted moving average.

**System Performance**

For an assessment of the performance of the system, reference can be made to Coatsworth and Hobbs [2] who carried out advanced tests to provide design parameters for a variety of construction projects. Their tests are summarized below.

*Stress Path Testing*

In situ ground deformation parameters were required for predicting the movement of a proposed immersed tube tunnel river crossing in Wales. Stress path tests were carried out on selected piston samples of glacial lake clays from beneath the proposed tunnel. As shown in Fig. 7, each test specimen was consolidated under a small all-round stress (point A in Fig. 7) to give it some stability. The specimen was then  $K_0$  consolidated to the maximum



A-B	$K_0$ consolidation	Representing geological history
B-C	Drained stress path	
C-D	Undrained unloading	Representing excavation of the trench
D-E	Swelling	
E-F	Undrained loading	Representing the placing of the immersed tube tunnel
F-G	Consolidation	
G-H	Undrained loading	
H-I	Consolidation	
I-J	Undrained loading	
J-K	Consolidation	
K-L	Undrained compression to failure	To determine the soil strength after construction

FIG. 7—Stress path test on glacial clay (from Coatsworth and Hobbs [2]).

previous consolidation pressure (stage A–B in Fig. 7). The final stage in the reimposition of the in situ stresses was to impose a drained stress path while allowing swelling to occur (stage B–C). The specimen was then subjected to undrained unloading to simulate excavation (stage C–D). Drainage was then allowed to occur at constant total stresses (stage D–E). The increments in vertical stress corresponding to tunnel construction were applied in a number of undrained stages, usually three (E–F, G–H, I–J), each undrained stage being followed by a drainage interval (F–G, H–I, J–K) during which the total stresses were maintained constant.

These tests provided deformation moduli significantly different from those obtained from conventional oedometer tests, even allowing for Skempton and Bjerrum's [7] correction, a general conclusion also reached by Simons and Som [8] who tested London clay.

### *Cyclic Loading Tests*

A series of tests were performed to model the behavior of normally consolidated sand below the center of a foundation subjected to repeated loading. The breadth of the foundation was large compared to the depth of sand, and so conditions of zero lateral strain were assumed. As shown in Fig. 8, the loading sequence to model conditions below the foundation were simplified into three stages, zero lateral strain conditions being maintained for both loading and unloading paths, as follows:

- initial consolidation of the sand under effective vertical overburden pressure,
- application of the dead load of the structure and application and removal of the proof load, and
- repeated application and removal of the live load during operational life of the structure.

The tests were carried out on samples of gravelly medium and coarse sand from Monkey Island, Bray, Berkshire, England. For clarity, the results given in Fig. 8 are for selected cycle numbers only. The control algorithm was written by the authors.

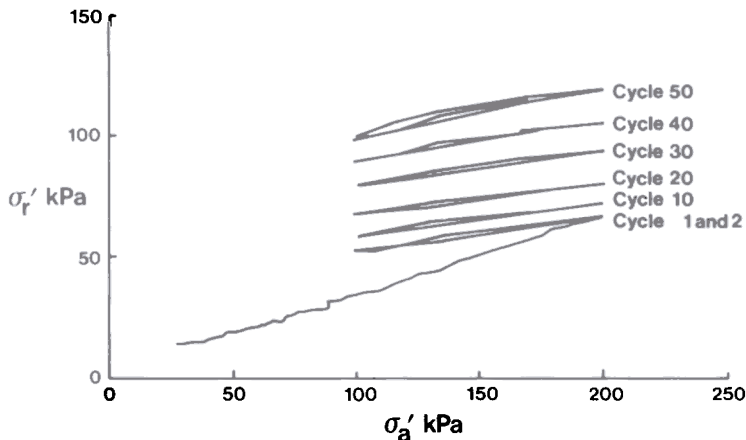


FIG. 8—Cyclic loading test on dense sand (from Coatsworth and Hobbs [2])

*Extension Tests*

A series of consolidated-undrained extension tests were carried out on overconsolidated silty clay to investigate the stability of the base of a deep excavation in the Middle East. The results of 1 set of tests on a stiff to very stiff silty clay overconsolidated by desiccation are given in Fig. 9 in which the strain contours show the mobilization of strength. In all, 24 tests were completed in 48 days with just 1 cell.

**System Features**

Some major features of the system are summarized below:

*Cell*

- Specifically designed to facilitate stress path testing
- Ram friction negligible and corrected for by computer anyway
- Plane top cap reduces bedding and alignment errors

*Digital Controllers*

- Pressure measured to 0.2 kPa, pressure controlled to 0.5 kPa
- Volume change measured and controlled to 1 mm<sup>3</sup>
- On-board intelligence enables ramping of pressure and volume change

*Software*

- Repeatability of tests
- Automatic data recording, data reduction, and data presentation to standard format
- Advanced tests can be carried out as routinely as conventional tests

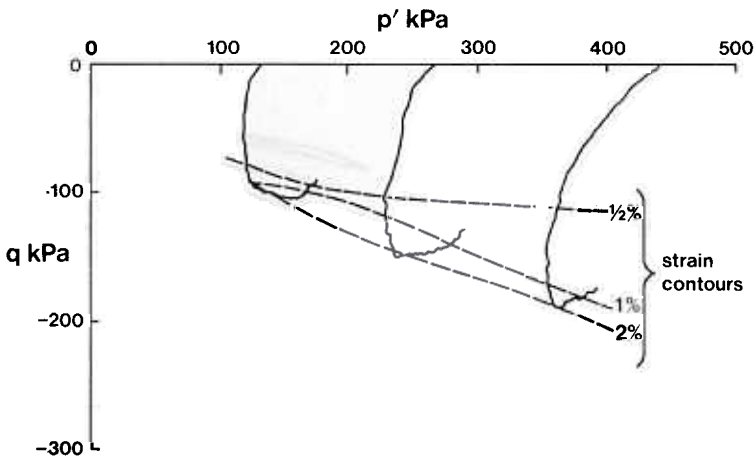


FIG. 9—Undrained extension tests on overconsolidated silty clay (from Coatsworth and Hobbs [2]).

Changing the triaxial cell for a hydraulic consolidation cell of the Rowe and Barden type [9] and changing the software package converts the system into a computer controlled consolidation testing system. The test menu includes classic step loading, constant rate of deformation, constant rate of loading, controlled hydraulic gradient, and permeability by constant rate of flow.

Because it is software based, the system repertoire may readily be updated to incorporate new techniques (for example, strain path testing) without changes in hardware. At the time of writing, over 50 systems are currently in use worldwide with the users providing an invaluable data bank of experience and suggestions. This feedback is reflected in periodic releases of software enhancements.

### *Acknowledgments*

The author thanks the editor of *Ground Engineering* and the directors of Soil Mechanics Ltd. for their permission to reproduce Figs. 7, 8, and 9.

### **References**

- [1] Menzies, B. K., "Soil Testing System," *Geotechnical News*, Vol. 1, No. 3, 1984, pp. 38-39.
- [2] Coatsworth, A. M. and Hobbs, N. B., "Computer Controlled Triaxial Soil Testing Equipment in a Commercial Laboratory," *Ground Engineering*, Vol. 17, No. 7, 1984, pp. 19-23.
- [3] Linenberger, M. J., "Microcomputer Controlled Cyclic Triaxial Testing System," Project Report NSF83-297p for Master of Science Degree, University of Massachusetts-Amherst, 1983.
- [4] Hsieh, K. H., "Techniques for Investigation of Sand Behaviour Under Cyclic Loading," Project Report OUR85-321p for Master of Science Degree, University of Massachusetts-Amherst, 1985.
- [5] Bishop, A. W. and Wesley, L. D., "A Hydraulic Triaxial Apparatus for Controlled Stress Path Testing," *Geotechnique*, Vol. 25, No. 4, 1975, pp. 657-670.
- [6] Olsen, H. W., Nichols, R. W. and Rice, T. L., "Low Gradient Permeability Measurements in a Triaxial System," *Geotechnique*, Vol. 35, No. 2, 1985, pp. 145-157.
- [7] Skempton, A. W. and Bjerrum, L., "A Contribution to the Analysis of Foundations on Clay," *Geotechnique*, Vol. 7, No. 4, 1957, pp. 168-178.
- [8] Simons, N. E. and Som, N. N., "Settlement of Structures on Clay with Particular Emphasis on London Clay," Report 22, CIRIA, London, 1970.
- [9] Rowe, P. W. and Barden, L., "A New Consolidation Cell," *Geotechnique*, Vol. 16, No. 2, 1966, pp. 162-170.